Journal of Structural Geology, Vol. 15, No. 12, pp. 1433 to 1441, 1993
Printed in Great Britain

0191-8141/93 $06.00+0.00

Subsolidus physical and chemical mixing of granite and gabbro during mylonitization, South Victoria Land, Antarctica

C. RACHEL WALCOTT and DAVE CRAW

Geology Department, University of Otago, P.O. Box 56, Dunedin, New Zealand

(*Received* 28 *October* 1991; *accepted in revised form* 7 *January* 1993)

Abstract—At Dromedary Massif, Southern Victoria Land, Antarctica, a suite of coarse-grained granite dykes cross-cuts a gabbro pluton which has been partially metamorphosed at amphibolite facies. During regional deformation, strain has been inhomogeneously distributed through the gabbro pluton and has been concentrated in granite dykes. In zones of relatively high strain, the granite dykes have developed a mylonitic fabric. A high strain gradient between granitic mylonite and metagabbroic host rock has induced isochemical mylonitization of the margin of the host. This grain size reduction allowed chemical diffusion between granitic and metagabbroic mylonites, resulting in a marginal zone of biotite-rich mylonite with intermediate composition. Biotite-rich mylonite decoupled from metagabbroic mylonite and flowed with granitic mylonite. Continued folding and transposition of granitic mylonite and biotite-rich mylonite has produced compositionally banded mylonite zones through thorough and irreversible mixing of the two lithologies.

INTRODUCTION

MYLONITES represent zones of high ductile strain in which the host lithology commonly undergoes grain size reduction. During deformation, the zone as a whole may remain isochemical (e.g. Kerrich *et al.* 1977, Wenk & Pannetier 1990) or undergo some chemical change due to fluid infiltration (Brodie 1980, Dipple *et al.* 1990, O'Hara 1990). On a smaller scale, deformation and recrystallization of homogeneous rock during mylonitization can cause segregation into layers of differing compositions (Robin 1979, Knipe & Wintsch 1985, Dipple *et al.* 1990). These layers are typically on the millimetre scale, and give rise to prominent banding in mylonites in hand specimen (Sinha Roy 1977). The banding is commonly tightly or isoclinically folded, and folds become progressively transposed with continuing strain. Segregation and mixing of rock elements are clearly an integral part of the deformation process in mylonite zones. Segregation is partly due to differential strain of minerals with contrasting strengths, such as quartz and feldspar (Wilson 1980), and some segregation and rehomogenization is due to chemical transfer (Wintsch & Andrew 1988, Dipple *et al.* 1990). However, the relative contributions of chemical and physical processes is difficult to determine in studies of mylonites derived from homogeneous parents. Further, the mechanisms of physical homogenization are poorly understood because of the lack of strong compositional distinctions. Study of mylonites developed in adjacent rocks of contrasting compositions can help to elucidate the processes of mylonitization, as deformation structures are shown up by original rock types.

In this study, we describe some rather spectacular mylonites developed in granite dykes cross-cutting metagabbro. Portions of metagabbro host have become incorporated into the mylonite zones, and deformed with the granitic mylonite. The very strong compositional contrast between the two lithologies involved make it easier to trace the physical incorporation of metagabbro into granitic mylonite. Because the end-member compositions are distinctive, the extent of chemical changes during mylonitization can be determined. This paper provides some field and geochemical evidence for the processes which result in formation of banded mafic and felsic mylonite. We focus on the physical mixing processes which occur during high strain of ductile rocks, and the extent of chemical changes which accompany that mixing.

GEOLOGICAL SETTING

In Southern Victoria Land, Antarctica, crystalline basement in the Transantarctic Mountains (Fig. 1) is composed of pelitic, psammitic and calcareous metasediments (Gunn & Warren 1962, Findlay *et al.* 1984). The basement has been intruded by mafic and felsic plutons and subsequently cross-cut by several suites of dykes during the early Paleozoic Ross orogeny. Regional strain during the Ross orogeny deformed basement and intrusives under amphibolite facies conditions and resulted in synmetamorphic disruption of many of the mafic plutons. Deformation was principally a result of E–W compression during W-directed subduction beneath the Gondwana margin (Borg *et al.* 1987). A metagabbro pluton which lies within Dromedary Massif (Fig. 1) in the Transantarctic Mountains hosts the rocks discussed in this paper. The pluton was intruded during the early stages of the Ross orogeny (Aslund 1990, Walcott 1990).

DROMEDARY METAGABBRO

The Dromedary metagabbro (Fig. 1) is a mafic intrusive complex which consists of both alkaline and tholeiitic cumulate and non-cumulate gabbros (Aslund 1990). The metagabbro complex is hosted by calcareous meta-

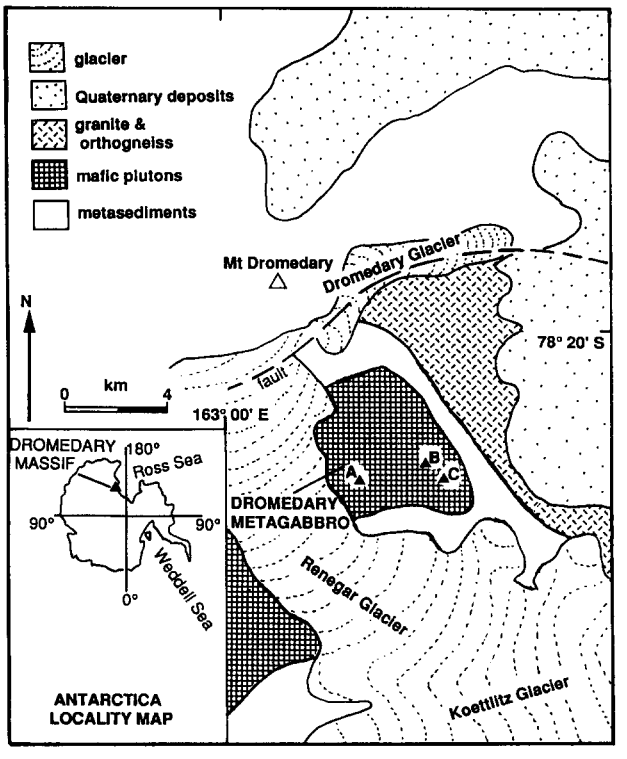

Fig. 1. Locality map showing the Dromedary metagabbro pluton, which host the mylonites discussed in this paper, intruded into amphibolite facies metasediments. The localities A, B and C described in the text are indicated with filled triangles.

sediments and crops out as a subelliptical body at least 4 km across and 6 km long. The body is made up largely of coarse-grained hornblende metagabbro, and primary pyroxenes and olivines are rarely visible in the weakly metamorphosed core zone of the body (Aslund 1990). A discontinuous outer zone of strongly foliated biotite-rich metagabbro occurs adjacent to host metasediments in zones up to 1 km wide.

Hornblende metagabbro, which is the immediate host rock for the mylonites discussed in this paper, consists of plagioclase (*ca* An_{50}) and hornblende (grains 0.5–2 cm) with minor biotite (Table 1). Quartz is rare, and occurs only as blebs in hornblende. Hornblende metagabbro is well lineated and weakly foliated. It is cut by brittle fractures, which are commonly developed along zones of ductile shear defined by alignment of hornblende long axes.

Metagabbroic mylonite zones 1–2 cm wide occur along the margins of mylonitized granite dykes (described below). Metagabbroic mylonite is composed of elliptical porphyroclasts of plagioclase distributed throughout a very fine-grained (0.2 mm) matrix of plagioclase, biotite, hornblende and magnetite (Table 1). The hornblende contains rounded quartz inclusions as in the metagabbro parent.

GRANITE DYKES

Undeformed dykes

Coarse-grained, pegmatitic granite dykes up to 3 m thick cross-cut metagabbro, the surrounding metasediment and neighbouring granite plutons (Fig. 1). Most undeformed dykes in the gabbro strike N–S and have moderate to steep dips, and appear to be part of a distinctive single swarm. The dykes are generally straight and parallel-sided. Irregularly-shaped metagabbro inclusions within dykes are rare. Disruption of some dykes has occurred within the gabbro, along brittle fractures. The dykes typically have a grain size greater than 1 cm and are composed of approximately equal proportions of quartz, potassium feldspar (up to 5 cm) and plagioclase (An_{20-30}), with minor biotite and tourmaline. Biotite occurs as rare clusters of grains with a low degree of preferred orientation, probably a pre-full crystallization fabric (Hutton 1988). Feldspars show no evidence of recrystallization, and quartz has only minor undulose extinction and localized minor subgrain formation. These microstructures are indicative of a very low degree of crystal plastic strain (Corrioux 1987).

Granitic mylonites

Deformation intensity is extremely variable within the gabbro pluton and its cross-cutting granite dykes. While much of the gabbro and some of the dykes are little deformed, many granite dykes which cross-cut gabbro, and the immediately adjacent gabbro, have been mylonitized (Figs. 2a & b). Three well exposed granitic mylonite localities were studied in detail (Fig. 1, localities A–C). The transition from relatively undeformed granite dyke into mylonitic granite is marked by a substantial grain size reduction, from typically >1 cm (see above) to typically <1 mm and a reduction in the width of dykes by 50% or more. Some dykes become progressively better foliated and finer grained along strike, and the transition from undeformed to mylonitic granite occurs over less than 2 m in some outcrops.

Granitic mylonite consists of quartz, plagioclase (An_{20-30}), potassium feldspar with minor biotite and tourmaline (Table 1). Granitic mylonite is texturally banded into coarse- and fine-grained layers and patches <1 cm in width (Fig. 2b), so modal proportions can be difficult to determine due to variability. The layering resembles the metamorphic segregation described by Sinha Roy (1977) and Robin (1979). Quartz occurs locally as elongate ribbons parallel to incipient foliation. Quartz ribbons vary from 2 × 0.3 mm down to 0.5 × 0.2 mm. Feldspar-rich domains are composed of polygonal grains (0.3 mm) and/or single subhedral grains (up to 2 cm long). The feldspar grains have similar dimensions to quartz ribbons. In the fine-grained layers (and in finer-grained mylonites) quartz occurs as polygonal and equant grains down to 0.2 mm in width. The matrix is composed of polygonal plagioclase and potassium feldspar grains (both ~0.3 mm), quartz and minor amounts of biotite. Porphyroclasts of potassium feldspar (0.5–2 cm) exhibit subgrain development, and annealing at their margins with minor myrmekite. Polygonal plagioclase grains (An_{20-30}) are typically 0.3 mm in diameter. Biotite, where present, is fine grained (<0.3 mm) and is aligned parallel to compositional layering. Apart from

Table 1. Geochemical analyses of Dromedary mylonites and parent lithologies

	SiO_2	TiO_2	Al_2O_3	FeO#	MnO	MgO	CaO	Na_2O	K_2O	LOI	Total	Ga	Rb	Sr	Y	Zr	Pb	Th	U
1. Gabbro*	48.30	0.55	18.00	12.00	0.17	6.80	8.80	2.30	1.40		98.32								
1. Gabbro	47.60	1.80	17.70	11.60	0.25	5.80	10.00	2.00	1.20	1.1	99.05	26	125	373	25	36	16	2	23
2. Gabbro	49.00	2.20	22.00	6.80	0.10	4.60	9.00	3.20	1.30	1.6	99.8								
3. Gabbro mylonite	47.10	2.40	18.50	11.50	0.20	5.20	10.00	1.80	1.20	0.8	98.74	19	103	265	26	23	15	0	5
4. Banded mylonite*	56.70	0.73	17.10	8.80	0.14	7.00	3.30	1.60	3.20		98.57								
5. Banded mylonite*	72.90	0.27	13.60	3.00	bd	2.60	3.90	1.90	1.20		99.37								
6. Banded mylonite*	66.20	0.32	17.20	3.60	bd	3.10	5.10	2.40	1.40		99.32								
7. Banded mylonite	67.40	0.70	15.00	4.80	0.10	2.30	4.00	2.90	2.00	1.3	100.5	19	214	121	66	57	18	14	25
8. Banded mylonite	61.70	0.90	16.00	6.20	0.10	3.00	5.70	2.00	3.00	1.1	99.7	21	135	231	49	46	18	16	4
9. Granite mylonite	76.90	bd	13.20	0.70	0.10	0.10	1.40	3.90	3.40	0.4	100.1	14	155	40	60	64	55	14	8
10. Granite mylonite	76.10	bd	13.30	0.60	bd	bd	0.50	2.90	6.00	0.4	99.76								
11. Granite dyke	75.60	0.10	13.50	0.65	bd	0.10	1.00	4.40	3.40	0.3	99.05	16	282	58	25	41	62	7	3
12. Granite dyke	76.80	bd	13.50	0.50	bd	0.10	1.00	3.40	4.70	1.4	101.4								
13. Granite dyke	76.10	0.07	13.90	0.60	bd	0.30	2.60	3.80	2.30	0.4	100.1								
14. Granite dyke	76.50	bd	13.00	0.40	bd	bd	0.80	2.90	6.00	0.2	99.79	17	299	9	24	33	69	4	2
Minerals, gabbro 1																			
Hornblende	50.50	0.76	11.90	9.18	0.32	11.20	12.60	0.97	0.54										
Biotite	37.50	1.60	18.00	17.70	0.30	15.40	0.00	0.10	7.0										

*Analyses calculated from modes. LOI=loss on ignition. FeO = all iron as ferrous. Oxides in weight percent; trace elements in parts per million.

the quartz ribbons, most microstructures indicate a substantial degree of post-deformation recrystallization. Grain size reduction around porphyroclasts and a well-defined foliation are the only indicators of deformation in many granite samples.

METAGABBRO INCLUSIONS

Inclusions of metagabbro, many with irregular shapes, are common in granitic mylonite, and most are elongate parallel to the mylonitic foliation (Fig. 3). Granitic mylonite apophyses up to 50 cm wide extend into the host metagabbro, sub-parallel to the deformed dyke margins. Similar, but smaller (1–10 cm) apophyses extend into metagabbroic inclusions. Coalescence of some apophyses separates blocks of metagabbro (up to 2 m long) from the host body or inclusions, and these detached blocks 'float' in granitic mylonite.

The granitic apophyses and enclosed metagabbro inclusions may be a result of molten granite dyke intrusion, but if so, the geometry has been considerably modified by subsolidus processes. A prominent mylonitic foliation in the apophyses lies parallel to the highly irregular metagabbro contact. A rim of metagabbroic mylonite, 0.5–2 cm wide, commonly occurs around the margins of metagabbro inclusions, parallel to the mylonitic foliation in the granite. Long narrow metagabbro inclusions have been folded at locality B into open warps, tight similar folds (locally refolded) and sheath folds (Fig. 3).

BIOTITE-RICH MYLONITE

The contact between granitic mylonite and metagabbroic mylonite is always marked by a zone of biotite-rich mylonite 0.5–2 cm thick (Fig. 2a). Biotite-rich mylonite has grain size similar to other mylonites, and consists of quartz (up to 40%), biotite and plagioclase (An_{30-40}). Some relict porphyroclastic plagioclase (up to 1 mm) has composition An_{40-50}. Grains of quartz, feldspar and biotite in the matrix of biotite-rich mylonite are polygonal and annealed, and biotite defines a prominent foliation which wraps around porphyroclasts. Potassium feldspar is rarely present in the biotite-rich mylonite, but commonly occurs on the diffuse boundary to granitic mylonite. Thus, biotite-rich mylonite has affinities to both the adjacent mylonites, but has closest affinities to the metagabbroic mylonite.

BANDED MYLONITE

Biotite-rich mylonite also occurs as thin (1 cm) but continuous layers within granitic mylonite zones, giving the rock a strikingly banded appearance. This compositional banding is distinct from localized quartz–feldspar compositional banding described above. The margin between biotite-rich mylonite and granitic mylonite is diffuse on the hand specimen scale (Fig. 2c), but well defined on the thin section scale (Fig. 2d). Metagabbro inclusions, with metagabbroic mylonite and biotite-rich mylonite rims, occur within granitic mylonite zones, adding to the banded appearance. Biotite-rich mylonite 'tails' extend away from the thinner parts of metagabbro inclusions into granitic mylonite. The 'tails', and associated metagabbro inclusions, are commonly tightly folded and sheath folds occur on all scales from centimetres to metres (Figs. 2c and 3). Folds have the annealed mylonitic foliation as a form surface, but this foliation has been transposed in minor fold hinges (Figs. 2c & d). Foliation in tightly folded 'tails' of biotite-rich mylonite is also locally transposed parallel to the main mylonitic foliation, and boundaries of these 'tails' become progressively more diffuse with distance from the

source metagabbro (Fig. 3). We interpret the biotite-rich mylonite in banded mylonite to be remnants of mafic mylonite from granite–gabbro contacts.

GEOCHEMISTRY OF MYLONITES

Analytical methods

Geochemical data were obtained from samples from locality C (Fig. 1), where a well-defined parallel-sided, parallel-foliated granitic mylonite 1 m wide cuts weakly foliated hornblende metagabbro. A sample of granitic mylonite, two samples of biotite-rich mylonite within the granitic mylonite, and a single sample containing undeformed metagabbro, metagabbroic mylonite and biotite-rich mylonite (Fig. 2a) were selected in a transect across the outcrop. Microprobe analyses were obtained for minerals in these samples. Hornblende and biotite compositions are consistent in all samples, and representative analyses are presented in Table 1. Plagioclase compositions are depicted in Fig. 4. X-ray fluorescence analyses of splits from *ca* 300 g pieces of these samples are presented in Table 1, along with analytical data for nearby host metagabbro and undeformed granite dykes. Biotite-rich mylonite material is internally inhomogeneous, so analytical data represent an average composition only. An attempt was made to further refine major element compositions of constituent layers by obtaining point count modes (Table 2) of distinct layers on the thin section scale. Modes were then combined with mineral densities and microprobe analyses of minerals into geochemical analyses of individual layers. This technique was checked by application to the adjacent undeformed metagabbro, and results are comparable to the XRF analysis (Table 1).

Results

The metagabbroic mylonite on the margin of the mylonite zone has very similar major and trace element composition to that of the adjacent metagabbro host. This is in accord with the similar mineralogy of these two rocks (Table 2). Likewise, the analysed leucocratic layer in the mylonite zone is very similar in composition to the parent granite dyke material from which it was derived.

Biotite-rich mylonite has petrographic affinities to metagabbroic mylonite, particularly with respect to feldspar textures, and compositions. The biotite-rich mylonite analyses show compositions which lie intermediate between the granite and gabbro end-members, for all elements analysed. This is shown best by major and trace elements which have the greatest differences between granite and gabbro (Fig. 5), although variability of granite specimens make definition of a leucocratic end-member difficult. Aluminium and iron contents of banded mylonite reflect the intermediate mafic and anorthite contents of the analysed material, both in bulk and in finer layers (from modal analyses). Potassium is more variable due to variable potassium feldspar contents in coarse-grained undeformed granite samples, but the same intermediate chemistry is indicated. The intermediate Sr content is in accord with the intermediate calcium content of the banded mylonite. Zr and Y are commonly considered to be 'immobile' elements, so the intermediate contents of these elements probably reflects the physical interlayering of mafic and felsic zones in banded mylonite (Fig. 2a).

Discussion of geochemistry of banded mylonites

Whole-rock compositions of biotite-rich mylonite lie between those of adjacent granitic mylonite and metagabbroic mylonite. Feldspar compositions also reflect this same intermediate chemistry. The presence of plagioclase porphyroclasts, and general absence of potassium feldspar from most biotite-rich mylonite, suggests that biotite-rich mylonite has formed primarily from metagabbroic mylonite due to elemental mobility during deformation of two lithologies of differing composition. Biotite and quartz have replaced hornblende in metagabbroic mylonite in response to influx of potassium and silica from the adjacent granitic mylonite. Biotite is more hydrous than hornblende, so some incursion of water may have occurred also, possibly from crystallizing granite. Localized biotite-rich zones, along the diffuse boundary between granitic mylonite and biotite-rich mylonite, contain some potassium feldspar porphyroclasts. These zones presumably represent altered granite, into which migration of iron and magnesium has occurred. In this manner, the compositions of the original mylonites have tended to merge in the zone of banded mylonites. Rock inhomogeneity and lack of constraints on volume changes prevent quantification of the amounts of elemental mobility. The chemical exchange process was initially concentrated at the

Fig. 2. Photographs of mylonites in the Dromedary metagabbro. (a) Section across a metagabbro–granite dyke margin, showing undeformed metagabbro with coarse plagioclase (bottom), metagabbroic mylonite with plagioclase porphyroclasts (centre) and banded mylonite with alternate biotite-rich and biotite-poor zones (top). Biotite-rich banded mylonite has plagioclase porphyroclasts, while biotite-poor banded mylonite has potassium feldspar porphyroclasts. (b) Mylonitic granite dyke (locality B), with coarse potassium feldspar porphyroclasts in a matrix of recrystallized potassium feldspar, plagioclase, ribbon quartz and tourmaline. (c) Intimately mixed biotite-rich mylonite (dark) and granitic mylonite (light), in a slabbed float sample obtained from locality B (Fig. 1), showing complex folding and transposition of the mylonitic foliation. Large white porphyroclasts in biotite-rich mylonite are plagioclase; large white porphyroclasts in granitic mylonite are potassium feldspar. (d) Photomicrograph across a transposed dark layer in (c). Annealed quartz, biotite and plagioclase occur at the boundary between biotite-rich mylonite (centre-right) and granitic mylonite (upper-left and lower-right). Dark patch in upper left is potassium feldspar porphyroclast (in extinction) with minor myrmekite on its margin. Biotite-rich mylonite contains numerous annealed plagioclase grains (some are twinned); granitic mylonite contains rare plagioclase. The biotite-rich mylonite has biotite grains oriented parallel to the fold axial surface in a minor fold hinge, resulting in incipient transposition of the contact between mylonite types. Crossed polars.

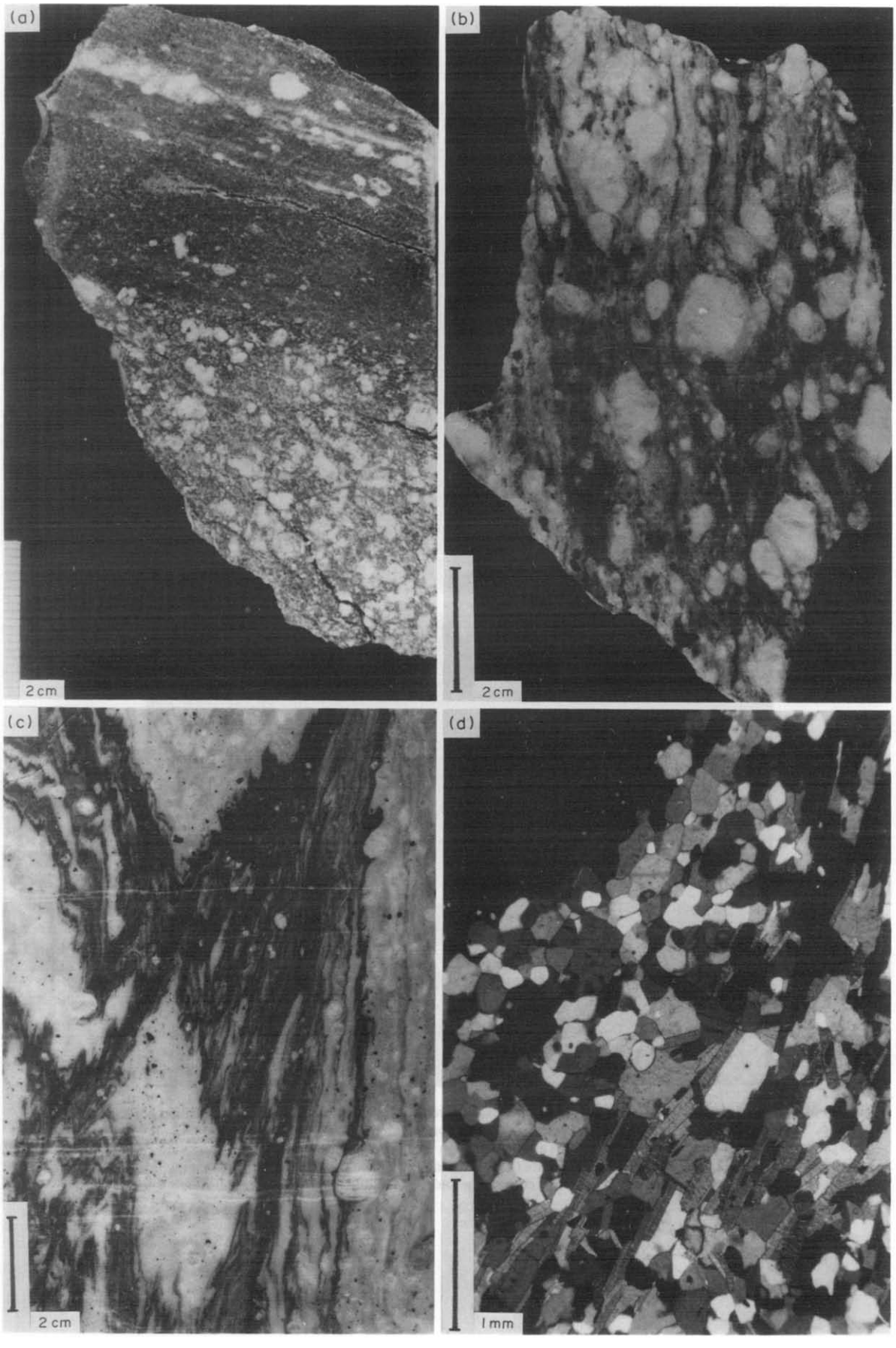

Fig. 2.

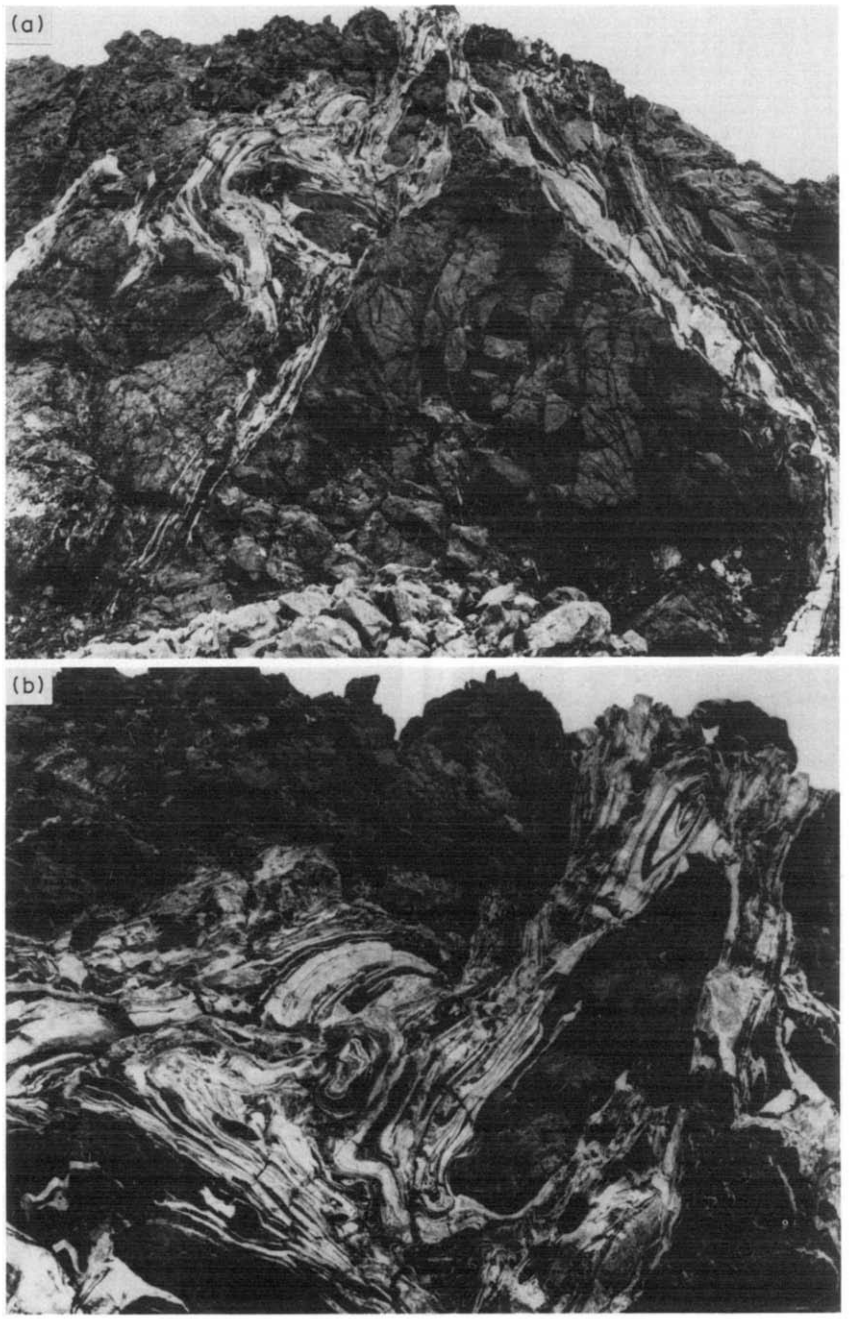

Fig. 3. Mylonitized granite dyke (light-coloured) in metagabbro (dark), at locality C (Fig. 1). (a) Photograph of the whole outcrop, showing the irregular thickness of the mylonite zone and the irregular margin with much interlayering of metagabbroic and granitic mylonite. Outcrop is about 30 m high on a near-vertical face. (b) Close-up view of the upper 10 m of the outcrop in (a). 'Tails' of biotite-rich mylonite (grey) stream away from metagabbroic mylonite inclusions, causing the prominent banding which has been complexly folded, including some mesoscopic sheath folds.

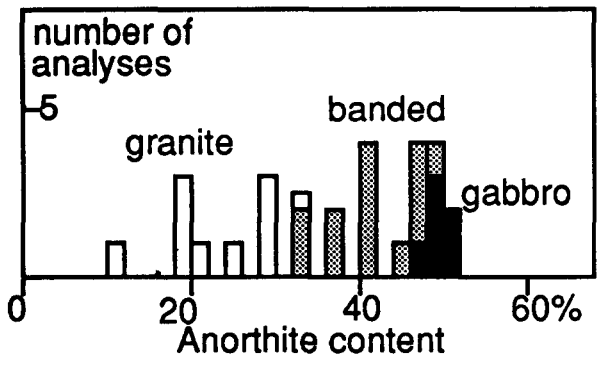

Fig. 4. Histogram of feldspar compositions (microprobe analyses) in undeformed granite and gabbro, and banded mylonite at locality C (Fig. 1).

margins of granitic mylonites, and at the margins of gabbroic inclusions in the granitic mylonite zones (Fig. 2a). Chemical diffusion would have been driven by chemical potential gradients between unlike lithologies, and enhanced by grain size reduction and recrystallization of the host gabbro and gabbro blocks.

The analytical data outlined above suggest that elemental mobility during mylonitization was restricted to scales on the order of 1 cm in regions where high chemical potential gradients existed during deformation. This scale of chemical mobility (centimetres) is small compared to the scale of the deformation zones (metres). The scale of chemical mobility is probably too small for complete formation of banded mylonite by chemical segregation, and some other process, presumably a physical process, has probably been involved in formation of the banded mylonite.

Development of banded mylonite implies physical separation of mafic mylonite from the margin of metagabbro, followed by physical interlayering of this mafic mylonite with granitic mylonite. Mafic mylonite which has been separated is invariably biotite-rich mylonite, so we infer that separation occurred only after metasomatic transformation of metagabbroic mylonite to biotite-rich mylonite. Some biotite-rich mylonite bands consist of partially or wholly metasomatized metagabbro inclusions in granitic mylonite (Figs. 2c and 3). Thin metagabbro protrusions from margins of inclusions or host, extending into apophyses of granitic mylonite, have been partially metasomatized, resulting in 'tails' of biotite-rich mylonite (Figs. 2c and 3). Mafic mylonite formed in these ways was surrounded by granitic mylonite and deformed with it. Physical mixing resulted from folding and transposition of biotite-rich mylonite during progressive strain of the granitic mylonite. This physical mixing process is probably a normal part of most mylonitization, but in this example, the mixing process is well displayed by the different rock types involved.

DISCUSSION AND CONCLUSIONS

Initial stages of mylonitization

Strain was initially concentrated in the granite dykes, and resulted in a mylonitic fabric which was later redeformed and annealed. This strain concentration may have arisen because the granite temperature was still high after intrusion, but the mylonite textures indicate that subsolidus crystal plasticity (White *et al.* 1980, Knipe 1989) was the dominant mechanism after granite crystallization (Hutton 1988). Alternatively, the presence of quartz which deforms readily under amphibolite facies conditions may have encouraged localization of ductile strain into granite rather than gabbro. Strain resulted in, and was accommodated by, ductile flow parallel to the wall of the dykes. The hornblende-rich, quartz-poor metagabbro did not undergo crystal-plastic processes initially, so brittle fractures developed in the metagabbro as a consequence of the regional strain and high viscosity contrast between granite and metagabbro. A very high strain gradient must have developed at the contact between the flowing granitic mylonite and relatively competent metagabbro. Initially, granitic mylonite and metagabbroic would have been decoupled, with relative movement at the boundary.

Development of biotite-rich mylonite

The high strain at the gabbro margin encouraged recrystallization, grain size reduction and softening of the metagabbro (Kirby 1985). Grain size reduction at the metagabbro margin encouraged some partitioning of the ductile strain into the metagabbro. Metagabbro grain size reduction encouraged more rapid elemental diffusion between mafic and felsic rocks, and biotite-rich mylonite formed. The resultant hybrid rock type contains quartz, plagioclase and biotite, and could deform via crystal plasticity with the granitic mylonite, in response to reaction softening (White *et al.* 1980). Granitic and biotite-rich mylonite viscosities presumably converged as their quartz and biotite contents converged. The two mylonite compositions resembled fluids of differing but broadly similar viscosities flowing together. The outlined processes represent coupling at the metagabbro margin of a migrating deformation front driven by the high strain gradient, and a migrating chemical diffusion front facilitated by decreasing grain size.

Mixing

Coupling between the biotite-rich mylonite and granitic mylonite allowed the biotite-rich mylonite to decouple from the wall rock and stream off into the granitic mylonite. Chemical diffusion may have persisted to further decrease the lithologic contrast between mafic and leucocratic layers.

Under high shear strain rates, deforming lithologies develop a shear-induced vorticity which can easily be converted into spin with changing boundary conditions or perturbations in flow within the deforming medium (Lister & Williams 1983, Bjornerud 1989). In banded mylonites the spin resulted in fold development. The structural complexity seen in Figs. 2 and 3 is the result of both high shear strain and the interference of folds produced from a large number of perturbations relative

Table 2. Modes (%) of mylonites and parent rocks

Sample	Gabbro 1	Gabbro 2	Gabbro 3	Banded 7 (dark)	Banded 5 (light)	Banded 8 (dark)	Granite 9	Granite 16	Granite 13
Quartz	1	1	3	22.5	46	32	39	43	29
K-feldspar	0	0	0	0	5	0	20	16	31
Plagioclase	42	65	34	33	33	49	39	36	37
Hornblende	36	12	41	0	0	0	0	0	0
Biotite	17	19	15	44	15	18	1	5	0
Magnetite	4	2	6	0.5	0	0	0	0	0
Tourmaline	0	0	0	0	0	1	1	0	3

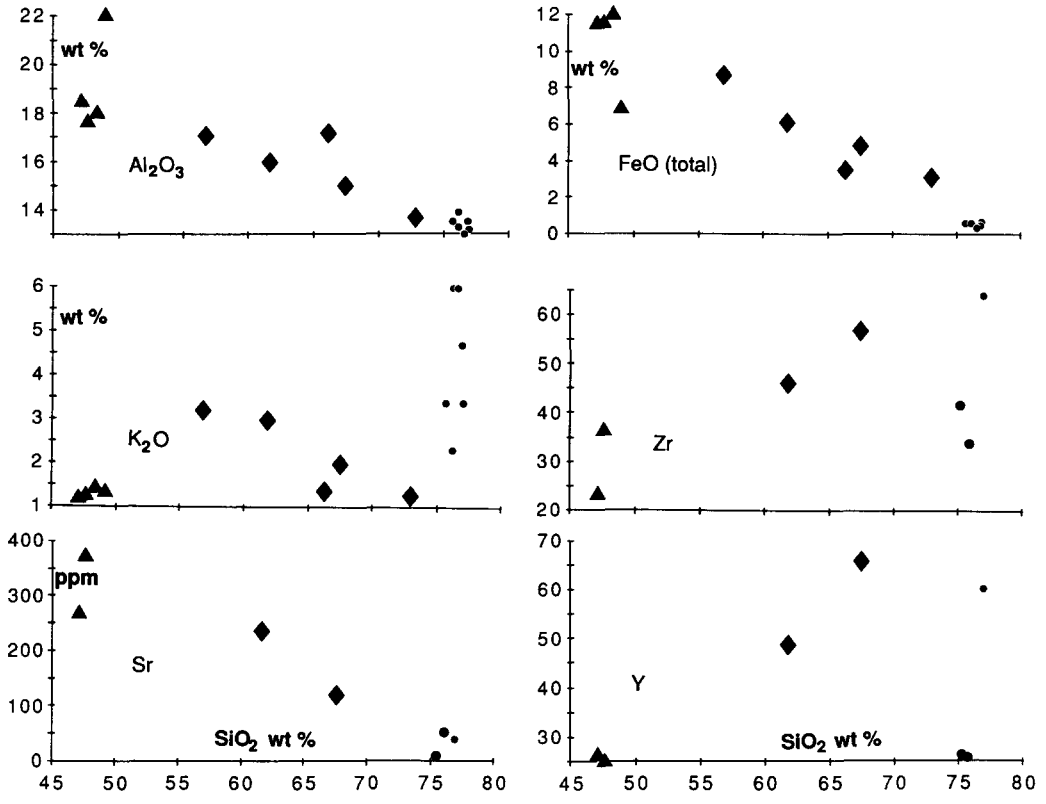

Fig. 5. Elemental variation diagrams comparing compositions of banded mylonite (diamonds) with metagabbro (triangles) and granite (dots). Horizontal axis is SiO_2 content in all diagrams, vertical axes show contents of selected elements from Table. 1, as indicated.

to the width of the deforming medium. The perturbations are provided by irregular host rock margins and angular relatively competent inclusions. Multiple folding, stretching and shearing is a typical mechanism for mixing of two fluids (Ottino *et al.* 1988), and we suggest that analogous processes occurred during formation of banded mylonites.

The physical mixing processes described above are scale-independent. The biotite-rich mylonite portion of banded mylonite becomes progressively more diffuse with increased strain and attenuation. This is probably due to operation of the chemical and physical mechanisms discussed above, at the boundary between mylonites of differing compositions. Ultimately, complete mixing and homogenization of banded mylonite might be expected down to even the scale of individual micaceous foliae. At the regional scale, deformation of metasedimentary belts between more competent plutons may involve similar processes. At this large scale, the effect of chemical homogenization would be expected to be relatively small (still on the centimetre scale), but could be significant if deformation caused lithological interlayering.

Acknowledgements—Field work for this study was financed by the New Zealand Universities Grants Committee and DSIR Antarctic Division. P. Garlick provided field assistance and photographs. Stimulating discussions with T. Aslund, S. C. Cox, P. O. Koons and R. J. Norris helped us to develop the ideas in the paper, but we remain responsible for errors in fact and interpretation. The manuscript was improved by thorough reviews from P.-Y. Robin and an anonymous referee. Technical assistance by R. D. Johnstone, J. Pillidge and D. Weston is gratefully acknowledged.

REFERENCES

Aslund, T. 1990. Metamorphism and magmatism of mafic intrusives at Dromedary Massif, Antarctica. Unpublished M.Sc. thesis, Otago University, Dunedin, New Zealand.

Bjornerud, M. 1989. Mathematical model for folding of layering near rigid objects in shear deformation. *J. Struct. Geol.* **11**, 245–254.

Borg, S. G., Stump, E., Chappell, B. W., McCulloch, M. T., Wyborn, D., Armstrong, R. L. & Holloway, J. R. 1987. Granitoids of

Northern Victoria Land, Antarctica: implications of chemical and isotopic variations to regional crustal structure and tectonics. *Am. J. Sci.* **287**, 127–169.

Brodie, K. H. 1980. Variation in mineral chemistry across a shear zone in phlogopite peridotite. *J. Struct. Geol.* **2**, 265–272.

Corrioux, G. 1987. Oblique diapirism; the Criffel granodiorite/granite zoned pluton (southwest Scotland). *J. Struct. Geol.* **9**, 313–330.

Dipple, G. M., Wintsch, R. P. & Andrews, M. S. 1990. Identification of the scales of differential element mobility in a ductile fault zone. *J. metamorph. Geol.* **8**, 645–661.

Findlay, R. H., Skinner, D. N. B. & Craw, D. 1984. Lithostratigraphy and structure of the Koettlitz Group, McMurdo Sound, Antarctica. *N. Z. J. Geol. Geophys.* **27**, 513–536.

Gunn, B. M. & Warren, G. 1962. Geology of Victoria Land between the Mawson and Mulock Glaciers, Antarctica. *Bull. N. Z. geol. Survey*. **71**.

Hutton, D. W. H. 1988. Granite emplacement mechanisms and tectonic controls; inferences from deformation studies. *Trans. R. Soc., Edinb.* **79**, 245–255.

Kerrich, R. & Allison, I. 1978. Flow mechanisms in rocks. *Geosci. Can.* **5**, 109–118.

Kerrich, R., Fyfe, W. S., Gorman, B. E. & Allison, I. 1977. Local modification of rock chemistry by deformation. *Contr. Miner. Petrol.* **65**, 183–190.

Kirby, S. H. 1985. Rock mechanics observations pertinent to the rheology of the continental lithosphere and the localization of strain along shear zones. *Tectonophysics* **119**, 1–27.

Knipe, R. J. 1988. Deformation mechanisms—recognition from natural tectonites. *J. Struct. Geol.* **11**, 127–147.

Knipe, R. J. & Wintsch, R. P. 1985. Heterogeneous deformation, foliation development, and metamorphic processes in a polyphase mylonite. In: *Advances in Geochemistry, Volume* 4: *Metamorphic Reactions* (edited by Thompson, A. B. & Rubie, D. C.). Springer, New York, 180–210.

Lister, G. F. & Williams, P. F. 1983. The partioning of deformation in flowing rock masses. *Tectonophysics* **92**, 1–33.

O'Hara, K. 1990. State of strain in mylonite from the western Blue Ridge province, southern Appalachians: the role of volume loss. *J. Struct. Geol.* **12**, 419–430.

Ottino, J. M., Leong, C. W., Rising, H. & Swanson, P. D. 1988. Morphological structures produced by mixing in chaotic flows. *Nature* **333**, 419–425.

Robin, P.-Y. 1979. Theory of metamorphic segregation and related processes. *Geochim. cosmochim. Acta* **43**, 1587–1600.

Sibson, R. H. 1977. Fault rocks and fault mechanisms. *J. geol. Soc. Lond.* **133**, 191–214.

Sinha Roy, S. 1977. Mylonite microstructures and their bearing on the development of mylonites—an example from deformed trondjemite of the Bergen Arc region, S.W. Norway. *Geol. Mag.* **144**, 445–458.

Walcott, C. R. 1990. The role of lithology during ductile deformation at Dromedary Massif Antarctica. Unpublished M.Sc. thesis, Otago University, Dunedin, New Zealand.

Wenk, H.-R. & Pannetier, J. 1990. Textural development in deformed granodiorite from the Santa Rose mylonite zone, southern California. *J. Struct. Geol.* **12**, 177–184.

White, S. H., Burrows, S. E., Carreras, J., Shaw, N. D. & Humphreys, F. J. 1980. On mylonites in ductile shear zones. *J. Struct. Geol.* **2**, 175–187.

Wilson, C. J. L. 1980. Shear zones in a pegmatite: a study of albite–mica–quartz deformation. *J. Struct. Geol.* **2**, 203–209.

Wintsch, R. P. & Andrews, M. S. 1988. Deformation induced growth of sillimanite: "stress" minerals revisited. *J. Geol.* **96**, 142–161.